The Kinetics of Oxidation of Iron-Silicon and Iron-Aluminum Alloy Melts by Pure Oxygen or Oxygen-Bearing Gases

T. EMI AND R. D. PEHLKE

The kinetics of oxidation of Fe-Si and Fe-Al melts by pure oxygen, and that of pure Fe by $He-O_2$, N_2-O_2, or $Ar-O_2$ mixtures have been investigated by a modified Sieverts' method at 1600°C. Considerable decrease in the oxidation rate has been observed for the alloy melts containing a few percent of Si or Al since formation of a silica- or alumina-rich oxide layer on the melts prevents further progress of the exothermic chemical reaction. The oxidation rate for melts high in Al has been considered to be limited by the diffusion of ions through the oxide layer. Addition of diluents to O_2 markedly and continuously decreases the oxidation rate of a pure Fe melt. The latter rate has been show to be controlled by the diffusion of O_2 across the gaseous boundaries at gas/melt interfaces.

THE remarkable developments of basic oxygen steelmaking processes in the last decade have generated considerable interest in the kinetics of reactions between gaseous oxygen and liquid iron alloys. The kinetics have also attracted much attention because they bear a close connection with problems arising from stream-reoxidation.

Many experimental and theoretical studies have been conducted on the kinetics of oxidation of carbon in liquid iron alloys, whereas only a few are available on that of liquid iron alloys containing deoxidizing elements such as silicon and aluminum. The latter studies are considered important to better understanding of stream-reoxidation of steels during teeming. Oxidation of iron-silicon alloys was studied by Filippov and Martynov[1] and by R. Baker.[2] The latter oxidized free falling droplets containing up to 7 pct Si at 1600°C by pure oxygen, and found that drops containing less than 6 pct Si burned extremely brightly and became covered with a thick layer of brittle scale while a passive film was formed on drops containing more than 6 pct Si resulting in the cooling of the drops during their fall. Baker's experiments were aimed at simulating spray refining processes, and detailed discussion of the kinetics was not given. Kaplan and Philbrook[3] oxidized levitation-melted samples of iron-silicon alloys by mixtures of 5 or 10 pct oxygen in helium at 1850 to 2050°C, and observed a temperature increase of the samples during the first seconds of the oxidation period and then a rapid temperature decrease which may have been due to the increase in the emissivity of the samples caused by slag formation. Further details of the experimental results were not reported. Kawai and Mori[4] also studied oxidation of silicon in iron by a carrier gas method with argon-hydrogen-water vapor mixtures at 1620 to 1710°C. Sano and Matsushita studied the oxidation of iron-silicon alloys in gas mixtures of CO_2 or O_2 with He as a diluent at temperatures from 1550 to 1800°C. They found the formation of solid or liquid oxide at lower temperatures was explained by diffusion of oxygen ions through the oxide layer. Experiments with $He-O_2$ mixtures were limited, however. The oxygen partial pressure of the mixtures was very low. Robertson and Jenkins[6] carried out more comprehensive experiments by oxidizing levitation-melted droplets of iron-silicon alloys in pure oxygen or gas mixtures containing 10 or 20 pct oxygen with argon as a diluent. They followed the course of reaction by a cinematographic technique and determined functionality of burning- or passive-behavior of the reaction with oxygen pressure and alloy compositions. They observed, as did Baker,[2] that passive behavior arose when a liquid slag layer approaching 50 μ in thickness formed during the first seconds of reaction at 1600°C and subsequently acted as a barrier to further rapid oxidation of the alloy. On the other hand, slags containing less silica did not so act during burning reactions and rapid oxidation ensued. In the above investigations, neither experimental set-up produced data of high accuracy, nor were the transient experimental conditions sufficiently clarified to allow one to determine kinetic parameters. Furthermore, no published data are available on oxidation of iron-aluminum alloy melts.

The purpose of this study was to investigate rate-determining steps and to determine kinetic parameters of the oxidation of iron-silicon and iron-aluminum alloy melts as a function of alloy compositions and gaseous oxygen pressures, thus providing information useful in evaluating stream-reoxidation.

EXPERIMENTAL PROCEDURE

Alloys of desired composition were prepared by premelting pure iron (Ferrovac E, Fe ≧ 99.92, C and S < 0.005, O < 0.0009 pct), analytically pure aluminum (Al ≧ 99.9 pct), or extra pure silicon (Si ≧ 99.999 pct) in vacuum in a recrystallized alumina crucible. A known amount, V_{st} (nominally 360 cm^3 STP), of extra-dry oxygen gas (O_2 = 99.9+ pct) or premixed, high purity helium-oxygen, nitrogen-oxygen, or argon-oxygen gases* were pressurized in a storage bulb, volume

T. EMI is Senior Research Associate, Research Laboratories, Kawasaki Steel Corporation, Chiba, Japan. R. D. PEHLKE is Professor and Chairman, Department of Materials and Metallurgical Engineering, The University of Michigan, Ann Arbor, Michigan 48104.

Manuscript submitted April 8, 1974.

*Subsequently dried in a standard gas train.

V_r = 317 cm^3 STP, which was connected via a solenoid valve to a Sieverts' type reaction bulb.

A polished alloy sample, weight W ≅ 100 gm, was then melted at 1600°C under argon in a recrystallized alumina crucible (ID 32 mm) which was placed in the reaction bulb, the hot volume, V_b, of which was determined for each run to be about 85 cm^3 STP. The reaction bulb was subsequently evacuated of argon, and the solenoid valve was instantaneously opened, allowing the gas in the storage bulb to flow out and fill the closed system, *i.e.*, the storage bulb-reaction bulb enclosure.

The absorption rate of oxygen was monitored by automatically recording the decrease in the system pressure which was detected by a strain-gauge type differential pressure transducer attached to the storage bulb. Further details of the experimental apparatus and procedure are described elsewhere.[7]

RESULTS

Strip chart recordings of the pressure change indicated *two distinct stages* for the oxidation of pure iron melts by the gas mixtures and of alloy melts by pure oxygen gas. This also has been observed for the oxidation of pure iron melts by pure oxygen gas.[7]

The first stage occurred immediately after the introduction of gases onto the surface of the melts, and involved rapid exothermic chemical reaction between oxygen in the gases and the surface of the melts. The surface of the melts for (pure O_2)-(Fe-Al or Fe-Si alloys) and ($O_2 \geq 95$ pct in He, N_2, or Ar)-(Fe) systems was observed to be covered by an oxide film at the end of the first stage which lasted only a fraction of a second. For ($O_2 \leq 90$ pct in He, N_2, Ar)-(Fe) systems, formation of such a distinct oxide film was not clear by visual inspection. A subsequent second stage which exhibited much slower rates occurred when the melt temperature decreased to its initial value.

The pressure change during the entire period of absorption was converted by a regression analysis into polynomials of the form

$$v = V_i + V_S = V_i + q_1 t + q_2 t^2 + q_3 t^3 + q_4 t^4 + q_5 t^5 \quad [1]$$

where v is the total volume of O_2 consumed during a time period t; V_i, the volume of O_2 absorbed in the first stage; V_S, that absorbed in the second stage, all in cm^3 STP; and q's are constants. The values of V_i and V_S thus calculated are summarized in Table I together with experimental conditions.

The dependence of V_i on the initial concentrations of alloying elements in the melts and those of diluents in the gas mixtures is shown in Fig. 1. The effect of Si on V_i was negligible up to 3 pct, then became significant around 4 pct beyond which a marked decrease of V_i was observed. Similarly, addition of Al up to 5 pct

Table I. Experimental Oxidation Data Obtained by a Modified Sieverts' Method at 1600°C

No.	A (cm^2)	Systems	V_b	V_r	P_r	V_i	$v = V_i + q_1 t + q_2 t^2 + q_3 t^3 + q_4 t^4 + q_5 t^5$				
							q_1	q_2	q_3	q_4	q_5
Si-4	8.1	(Fe-0.50 pct Si)-(pure O_2)	85.3	317.0	939	191.0	5.011	−0.07020	3.800×10^{-4}		
Si-3	7.8	(Fe-1.00 pct Si)-(pure O_2)	83.2	317.0	947	198.8	4.433	−0.05724	2.713×10^{-4}		
Si-9	7.6	(Fe-1.00 pct Si)-(pure O_2)	87.0	317.0	945	187.1	5.244	−0.06510	2.943×10^{-4}		
Si-5	7.7	(Fe-1.99 pct Si)-(pure O_2)	83.9	317.0	953	191.6	3.237	−0.02585			
Si-2	7.9	(Fe-2.89 pct Si)-(pure O_2)	81.5	317.0	956	198.6	1.556	−0.01687			
Si-7	8.0	(Fe-4.31 pct Si)-(pure O_2)	85.5	317.0	942	50.2	0.575	−0.00113			
Si-6	7.8	(Fe-5.74 pct Si)-(pure O_2)	85.9	317.0	947	25.7	0.457	−0.00087			
Al-5	8.0	(Fe-1.0 pct Al)-(pure O_2)	87.1	317.0	938	152.7	5.860	−0.08505	6.253×10^{-4}	1.818×10^{-6}	
Al-4	8.0	(Fe-1.0 pct Al)-(pure O_2)	86.1	317.0	939	160.1	5.685	−0.07144	3.260×10^{-4}		
Al-1	7.7	(Fe-1.5 pct Al)-(pure O_2)	78.7	317.0	956	160.8	6.040	−0.08760	4.090×10^{-4}		
Al-3	8.0	(Fe-3.0 pct Al)-(pure O_2)	82.2	317.0	943	210.1	4.930	−0.07362	3.958×10^{-4}		
Al-6	7.9	(Fe-5.0 pct Al)-(pure O_2)	85.2	317.0	944	148.9	0.121				
Al-9	7.4	(Fe-6.5 pct Al)-(pure O_2)	85.3	317.0	948	119.9	0.317				
Al-10	8.5	(Fe-10 pct Al)-(pure O_2)	85.3	317.0	948	25.3	0.075				
He-3	7.9	(pure Fe)-(He-98.95 pct O_2)	85.0	317.0	948	80.7	6.320	−0.1181	1.337×10^{-3}	7.622×10^{-6}	1.669×10^{-8}
He-6	7.8	(pure Fe)-(He-95.05 pct O_2)	85.0	317.0	940	47.0	4.892	−0.0784	0.678×10^{-3}	2.839×10^{-6}	0.452×10^{-8}
He-5	7.8	(pure Fe)-(He-89.95 pct O_2)	86.0	317.0	942	40.7	1.604	−0.0120	0.051×10^{-3}	-0.113×10^{-6}	0.974×10^{-10}
He-7	7.8	(pure Fe)-(He-79.18 pct O_2)	86.0	317.0	947	20.2	0.892	−0.0059	0.021×10^{-3}	-0.037×10^{-6}	0.245×10^{-10}
N_2-1	8.5	(pure Fe)-(N_2-98.89 pct O_2)	85.0	317.0	939	92.0	4.538	−0.0640	0.498×10^{-3}	-1.890×10^{-6}	0.273×10^{-8}
N_2-9	8.3	(pure Fe)-(N_2-94.99 pct O_2)	85.0	317.0	935	62.4	2.112	−0.0157	0.069×10^{-3}	-0.153×10^{-6}	0.013×10^{-8}
N_2-8	8.7	(pure Fe)-(N_2-89.62 pct O_2)	84.1	317.0	936	41.8	0.751	−0.0020	0.003×10^{-3}	-0.152×10^{-8}	
N_2-7	8.1	(pure Fe)-(N_2-79.91 pct O_2)	85.0	317.0	936	20.9	0.423	−0.0010	0.129×10^{-5}	-0.064×10^{-8}	
N_2-2	8.0	(pure Fe)-(N_2-59.07 pct O_2)	85.0	317.0	944	17.2	0.235	−0.0009	0.233×10^{-5}	-0.064×10^{-8}	
N_2-4	8.0	(pure Fe)-(N_2-39.50 pct O_2)	85.0	317.0	952	12.0	0.152	−0.0006	0.128×10^{-5}	-0.104×10^{-8}	
N_2-6	7.9	(pure Fe)-(N_2-21.10 pct O_2)	85.0	317.0	930	7.9	0.103	−0.0002	0.136×10^{-6}		
Ar-5	8.6	(pure Fe)-(Ar-98.90 pct O_2)	85.0	317.0	945	98.6	0.403	−0.0542	0.412×10^{-3}	-1.537×10^{-6}	0.218×10^{-8}
Ar-6	8.1	(pure Fe)-(Ar-95.11 pct O_2)	85.0	317.0	935	44.6	1.946	−0.0165	9.575×10^{-5}	-0.298×10^{-6}	
Ar-4	8.3	(pure Fe)-(Ar-90.06 pct O_2)	81.2	317.0	945	41.8	0.762	−0.0022	0.321×10^{-5}	-0.172×10^{-8}	
Ar-7	7.9	(pure Fe)-(Ar-79.76 pct O_2)	85.0	317.0	924	20.1	0.523	−0.0020	0.484×10^{-5}	-0.588×10^{-8}	0.280×10^{-11}
Ar-3	8.0	(pure Fe)-(Ar-58.47 pct O_2)	85.0	317.0	937	7.4	0.167	−0.0004	0.367×10^{-6}		
Ar-2	8.0	(pure Fe)-(Ar-39.78 pct O_2)	85.0	317.0	950	4.9	0.050	-8.5×10^{-5}	0.547×10^{-3}		
Ar-1	8.1	(pure Fe)-(Ar-20.96 pct O_2)	85.0	317.0	947	3.5	0.038	-9.5×10^{-5}	0.115×10^{-6}	-0.525×10^{-10}	

A is surface area of the melts, V_b and V_r are the volume of reaction bulb and storage bulb, respectively, in $STPcm^3$, P_r is the pressure of gases initially stored in the storage bulb in mmHg. v is the total amount of oxygen consumed during the first and second stages of oxidation, V_i is that consumed during the first stage, both in $STPcm^3$, and t denotes time of reaction for the second stage in s.

decreased V_i only slightly compared to a sudden decrease in V_i beyond about 7 pct.

On the other hand, the dilution of O_2 with He, N_2, or Ar caused a steep but continual decrease in the value of V_i for pure iron melts. It is to be noted that even a 1 pct addition of these diluents decreased V_i by almost one half of that for pure O_2. The extent of the change was, within the experimental error, alike for the three mixtures up to a diluent concentration of 20 pct.

The rate of absorption, dV_S/dt, of O_2 in the second stage followed the same trend as above, although a steep fall of dV_S/dt took place at lower concentrations of Si or Al, over a range of 1 to 4 pct for Si and 4 to 6 pct for Al, and at higher concentrations of the gaseous impurities. An example is shown in Fig. 2 where, as in Fig. 1, the abscissa indicates initial concentrations of the alloying elements.

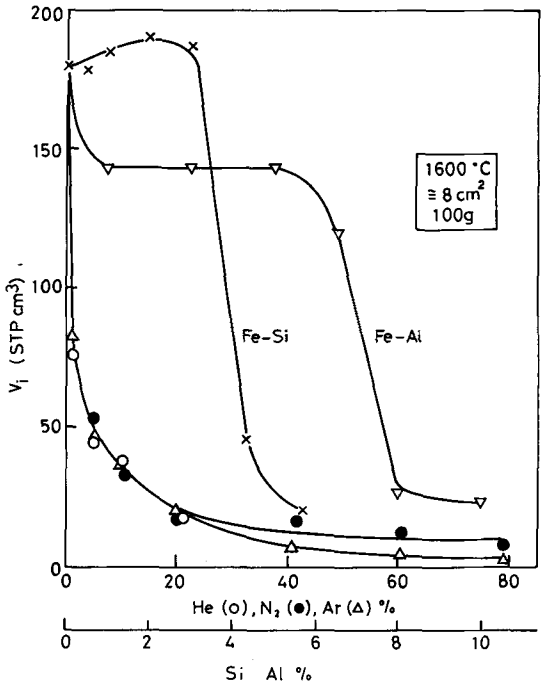

Fig. 1—Effect of the concentration of alloying elements and gaseous diluents on V_i.

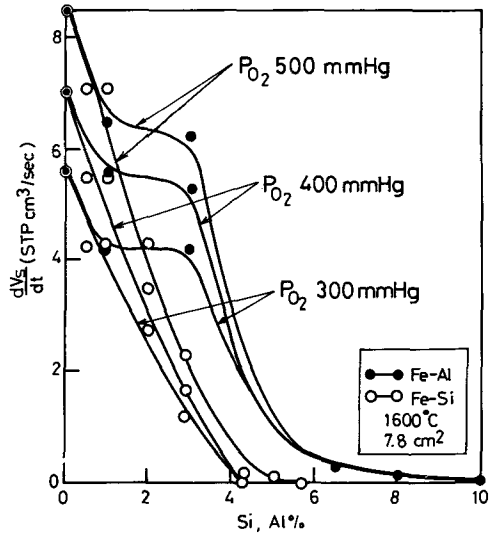

Fig. 2—Effect of the concentration of alloying elements on dV_S/dt.

These observations, together with the effect of the gaseous impurities on dV_S/dt for pure iron melts, will be discussed in the following paragraphs.

DISCUSSION

The overall oxidation reaction involves the following steps: a) transport of oxygen from the bulk gas to the gas/metal interface, b) chemical reaction at the interface to form dissolved oxygen and/or oxides, and c) transfer of dissolved oxygen to the bulk melt and/or the growth of the oxides at the interface.

In the first stage, a decrease of the system pressure, which was caused by the instantaneous exothermic chemical reaction taking place upon the introduction of pure oxygen to the reaction bulb, was too rapid to be followed by the pen-recorder employed in this study. The behavior of the pressure change was further complicated for the gas-mixtures by thermal expansion of the inert-gas components. For these reasons, the progress of the oxidation reaction during this stage cannot be interpreted reliably, and hence, discussion will be confined only to the total volume, V_i, of oxygen consumed in the first stage.

It has already been shown in a previous paper[7] that V_i for the (pure O_2)-(Fe) system involves contributions both of step b) to form iron oxides and of c) to grow the oxide layer. The value of V_i observed in the present experiments for the (pure O_2)-(Fe-Si) system containing up to 3 pct Si exhibited, as shown in Fig. 1, roughly the same value as that for the (pure O_2)-(Fe) system. This indicates that the formation and growth of an iron oxide layer on the surface of iron-silicon alloys were not significantly affected by the presence of Si up to 3 pct, *i.e.*, enrichment of silica in the iron oxides formed was not marked when silicon concentrations in the melt were limited. For higher silicon concentrations, however, selective oxidation of silicon took place to form a silica-enriched oxide layer on the melt surface. The viscous iron-silicate layer sharply diminished further growth by lowering the diffusivity of ions in the oxide layer. This explains the sudden decrease of V_i for the (pure O_2)-(Fe-Si) system at about 4 pct Si. It is interesting to note that this decrease of V_i agrees very well with the transition observed by Robertson and Jenkins[5] of reaction behavior from burning to passive at about 3.6 pct Si for (pure O_2)-(Fe-Si) systems at 1660°C (Fig. 3 of Ref. 6. It is also interesting in this regard that silicon removal curves reported by Baker[2] for oxidation of 2 mm diam. Fe-Si alloy droplets exhibited, as shown in Fig. 3, exactly the same behavior as the V_i curve for Fe-Si alloy melts determined in the present study (Fig. 1). The silicon removal curve[2] clearly suggests initiation of selective oxidation above 3 pct Si which agrees remarkably well with the silicon concentration above which V_i shows a sharp drop. At 5 pct Si, V_i decreases to about 1/6 of that for pure iron, while $\Delta Si/Si$ of the silicon removal curve[2] at the same silicon concentration is about 1/5 of that for nearly pure iron.

Although experimental conditions in each of the above experiments were different, this good agreement shows

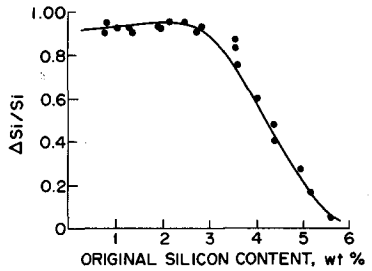

Fig. 3—Silicon removal from Fe-Si alloys (redrawn from Baker[2]).

that the initial period of the oxidation of iron-silicon alloys is predominantly controlled by the properties of slag films formed on the surface of the melts. The higher the silicon concentration in the melts, the more the oxide layer is enriched in silica. This results in a diminution of the growth rate of the layer, and hence a lower value of V_i. The behavior of V_i in the (pure O_2)-(Fe-Al) system is quite similar to that of the (pure O_2)-(Fe-Si) system, although a slight decrease in V_i is observed at low aluminum concentrations (Fig. 1).

On the other hand, steps b) and c) may not be the rate-determining steps for the oxidation of pure iron by the gas mixtures, because V_i for the mixtures with 99 pct O_2 was less than one-half of that for pure oxygen, the oxidation by which is known to be limited by step b) as well as c). With the same experimental conditions, the dilution of oxygen by addition of 1 pct inert gas may not explain such a drastic decrease of V_i for pure iron melt if steps b) and c) are also contributing equally to limit the first stage of oxidation by the gas mixtures. Instead, it appears reasonable to assign step a) to the rate-controlling step of the oxidation by the gas mixtures. Owing to the rapid consumption of oxygen in the early period of the first stage, the layer of gases in contact with the melt surface becomes instantaneously enriched with an inert-gas component of the mixture to develop a gaseous boundary layer which prevents further rapid transfer of oxygen from the bulk gas to the gas/metal- or, in the case where oxides are already formed, to the gas/oxide-interface.

In the second stage, where the surface temperature resumes approximately its initial value, oxidation proceeded at rates which could be monitored continuously and which offer a basis for interpretation of reaction behavior.

Rate-Controlling Steps for the Oxidation of Binary Alloy Melts by Pure Oxygen

The kinetics of oxidation of pure iron by pure oxygen in the second stage have been shown[7] to be described by the equation

$$\frac{dv}{dt} = \frac{dV_s}{dt} = Ak_1(P^b_{O_2})^{1/2} \qquad [2]$$

where k_1 is the specific reaction rate constant, A is the interfacial area, and $P^b_{O_2}$ is the instantaneous pressure of oxygen in the closed system when dv/dt is determined. In Eq. [2], zero time for the second stage is taken to be the end of the first stage which can be clearly distinguished on the strip chart recording of the system pressure.[7]

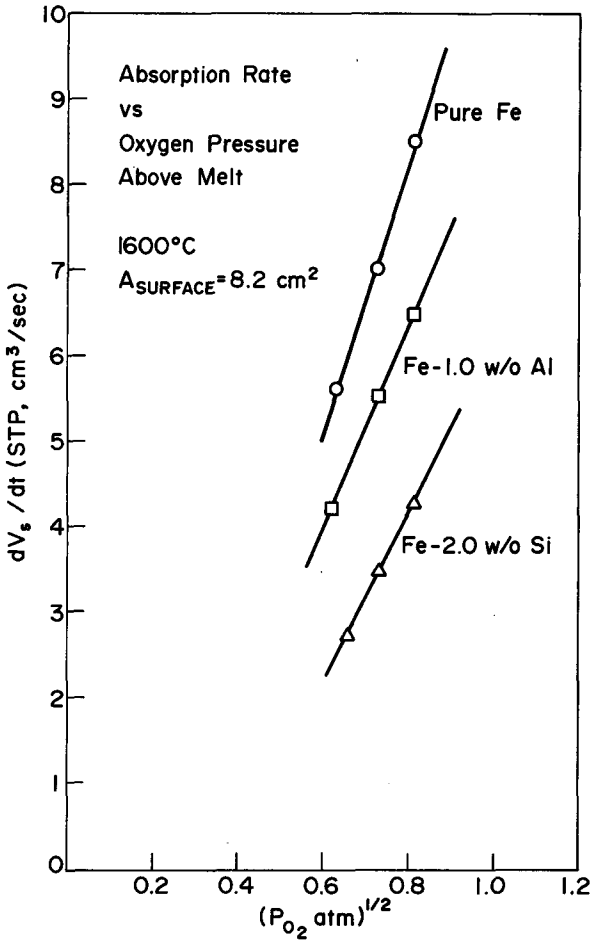

Fig. 4—Rates of oxygen absorption during second stage as a function of instantaneous system pressure.

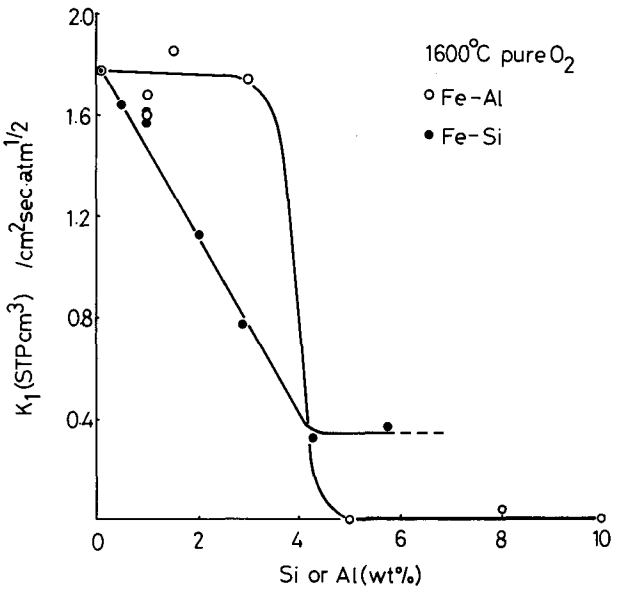

Fig. 5—Rates of oxidation of binary iron melts by pure oxygen gas.

A good linear relationship is obtained between $(1/A) \cdot (dv/dt)$ and $(P^b_{O_2})^{1/2}$ for the alloy melts under investigation, as shown in Fig. 4. Thus, k_1 serves to describe the change of oxidation rate with concentration of alloying element. This is shown in Fig. 5, where the ab-

scissa indicates initial concentration of the alloying elements.

The rate-controlling step for the second stage oxidation, which follows Eq. [2], of a pure iron melt by pure oxygen gas has been shown[7] to be the growth of the surface oxide layer by dissociative adsorption of oxygen molecules at the gas/oxide interface, O_2(gas) $\rightleftharpoons$ O_2(physisorbed) $\rightleftharpoons$ 2O (chemisorbed), followed by incorporation of the adsorbed oxygen atoms into the oxide, O(chemisorbed) $\rightarrow$ O(incorporated). The values of k_1 for Fe-Si and Fe-Al melts up to 1 pct Si and 3 pct Al are close to k_1 for pure iron, hence the above step is considered to control the rate for these melts too. On the other hand, the marked decrease of k_1 for Fe-Si and Fe-Al melts beyond the above mentioned concentrations of Si and Al indicates that a slower process for the growth, presumably the diffusion of ions through the oxide layer, becomes dominant. Namely, iron oxides are, with increasing concentration of the alloying elements in the melts, gradually enriched with silica or alumina produced by the selective oxidation of the corresponding alloying element. The transference number of electrons and ions in the silica- or alumina-enriched oxide layer becomes correspondingly different from that in iron oxides. In an extreme case, almost pure silica or alumina may constitute the surface oxide layer, inhibiting any further oxidation of the melts by retarding considerably the diffusion of ions across the layer. This perhaps was the case for Fe-Si (Si $\geqq$ 4 pct) and Fe-Al (Al $\geqq$ 5 pct) melts for which practically pure silica and alumina were respectively identified on the surface of quenched melts.

If so, taking into account the fact that the dependency of the rate on $P^b_{O_2}$ could be neglected in the above instances since the rate was too small to cause noticeable decrease in $P^b_{O_2}$, a parabolic growth formalism[8] which includes the transference number of ions should apply to the growth of the oxide layer as

$$v^2 = (700A)^2(k_2 t + Q) \qquad [3]$$

where

$$k_2 = \frac{d_{M_aX_b} kTM_X^2}{N_A e^2 z^2 M_{M_aX_b}} \int_{P^m_{O_2}}^{P^g_{O_2}} t_e(t_M + t_X)\gamma \, d \ln P_{O_2} \qquad [4]$$

and

$$Q = (V_i/700A)^2 \qquad [5]$$

where Q is the initial amount of oxide layer, and other terms are: d and M, density and molecular weight of subscript species; N_A, Avogadro's number; k, Boltzmann's constant; M_aX_b stands either for SiO_2 (a = 1, b = 2) or for Al_2O_3 (a = 2, b = 3); z, the valence of oxygen anion (2); e, the charge of an electron; t_e, t_M, and t_X, the transference number of electrons, metal ions, and oxygen anions, respectively; $P^g_{O_2}$ and $P^m_{O_2}$, oxygen pressures at gas/oxide- and metal/oxide-interface; and γ is the electrical conductivity of the oxide, M_aX_b. Differentiating and rearranging Eq. [3], one gets the following time independent rate of oxidation,

$$dv/dt \cong (A/2Q^{1/2})k_2 \qquad [6]$$

provided that the value of Q is sufficiently larger than that of $k_2 t$. This relation is actually observed in Table I for Fe-Al melts with more than 5 pct Al, *i.e.*, v for these melts is expressed by

$$v = V_i + V_S = V_i + q_1 t \qquad [7]$$

therefore

$$dv/dt = q_1 \qquad [8]$$

Thus, denoting q_1 to be equal to $(A/2Q^{1/2})k_2^{obs}$, one can compare experimentally obtained k_2^{obs} with theoretically calculated k_2 values from Eq. [4].

For alumina at 1600°C, γ is reported to be 3.1×10^{-5} $(\Omega cm)^{-1}$, t_e and $(t_M + t_X)$ do not depend on the pressure of oxygen and are 0.29 and 0.71, respectively,[9] ln $P^m_{O_2}$ is about -46, and Q can be obtained from Eq. [5] and V_i in Table I. The results of the calculation are summarized in Table II together with k_2^{obs} obtained from q_1's in Table I. For a Fe-10 pct Al melt, a large difference is observed between Ak_2 and Ak_2^{obs} in Table II. This, however, is not surprising in view of the fact that the value for Q for the melt is so small as to violate the reservation made on Eq. [6]. Except for this, the calculation seems to be consistent with the experimental observations and to support the postulation that diffusion of ions across the layer of alumina controls the rate of growth of the layer, hence the rate of oxidation of Fe-Al melts containing more than 5 pct Al.

The theory presented here is not capable of quantitative evaluation for Fe-Si melts containing more than 4 pct Si since a transference number has not yet been reported for silica at 1600°C. However, the linear decrease of k_1 in Fig. 5 for Fe-Si melts indicates that the composition of the surface oxide is continuously increasing in silica and, correspondingly in viscosity. The rate of transport of ions across the oxide layer decreases, resulting in a lower rate of oxygen gas consumption. On the other hand, the rate for Fe-Al melts exhibits a sudden decrease within a narrow concentration range at about 4 pct Al. This may reflect a change in the composition of the surface oxide from iron-rich to alumina-rich at this concentration. In all of the above discussions, the concentration of the alloying elements in the melts has been taken to be the initial concentration because the loss of the elements caused mainly by the first stage oxidation amounts, even with V_i of 190 cm^3 (STP) and assuming V_i to be totally expended to oxidize the elements, only to less than 0.3 pct of reacting alloying element.

Rate-Controlling Step for the Oxidation of Pure Iron Melts by Binary Gas Mixtures

The data in Table I are rearranged to determine the functionality of the variables $P^b_{O_2}$ and A with dv/dt for the oxidation of pure iron melts by He-O_2, N_2-O_2, and Ar-O_2 mixtures. A linear correlation between $(P^b_{O_2})^n$

Table II. Predicted Compared to Measured Parabolic Rate Constant for Oxidation of Iron-Aluminum Alloy Melts

Systems	Ak_2	Ak_2^{obs}
Fe-5.0 pct Al	0.12	0.12
Fe-6.5 pct Al	0.15	0.32
Fe-10.0 pct Al	0.70	0.08

vs. $(1/A)(dv/dt)$ is best represented by taking n equal to unity for the mixtures containing less than 85 pct O_2, whereas both n's of one-half and unity yield, with larger deviations, linear correlations between the two variables for the mixtures containing more than 85 pct O_2. In the case of pure O_2, n equal to one-half resulted in the best linear correlation between the two variables.[7] The change in n of one-half to unity clearly indicates that the rate-determing step changes with oxygen concentration. This can also be recognized in Fig. 6 in which an apparent rate constant k_3 defined by the relationship

$$dv/dt = Ak_3^{obs} P_{O_2}^b \quad [9]$$

is derived from Table I and plotted against oxygen concentration. It must be noted here that the term oxygen concentration in the gas mixtures is defined not as the initial concentration of oxygen stored in the storage bulb but as that in the reaction bulb (therefore in the closed system) at the time when dv/dt is determined. One may note in Fig. 6 that k_3^{obs} decreases sharply down to 85 pct O_2, then becomes constant below this composition. The value of k_3^{obs} for this constant portion is 0.26 for N_2-O_2 and Ar-O_2 mixtures, while 0.55 (STP cm^3)/($cm^2 s \cdot atm$) is obtained for He-O_2 mixtures.

These observations indicate that the transport of oxygen through the boundary layer within the gas phase containing less than 85 pct oxygen limits the rate of oxidation. The validity of this postulation is tested by comparing the observed values, k_3^{obs}'s, with those theoretically deduced as follows.

If the boundary layer transport is controlling the rate, one has

$$dv/dt = (AD^g/\delta_g)(P_{O_2}^b - P_{O_2}^m) = A(D^g/\delta_g)P_{O_2}^b = Ak_3 P_{O_2}^b \quad [10]$$

where D^g is the binary diffusivity for a gas mixture, and δ_g is the thickness of the gas film at the gas/oxide interface. The diffusivity can be estimated directly, *e.g.*, using equations and data tabulated by Hirschfelder, Bird and Spotz.[10]

Estimation of δ_g for the present experimental set-up seems rather difficult, but δ_g should be proportional to $(D^g t)^{1/2}$. One has then, with $D^g/\delta_g \propto (D^g/t)^{1/2}$,

$$k_3 \text{ for Ar-}O_2;\ k_3 \text{ for } N_2\text{-}O_2;\ k_3 \text{ for He-}O_2 = (D^g \text{ for Ar-}O_2)^{1/2};\ (D^g \text{ for } N_2\text{-}O_2)^{1/2};\ (D^g \text{ for He-}O_2)^{1/2} \quad [11]$$

at an identical time, provided that simultaneous absorption of N_2 in the melt can be neglected for N_2-O_2 mixtures.

The theoretical relationship, Eq. [11], is calculated and compared with experimental observations in Table III. The observed ratio, (k_3 for Ar-O_2)/(k_3 for N_2-O_2)/(k_3 for He-O_2) of 1/1/2.1 agrees within experimental error with the theoretically deduced ratio, (D^g for Ar-O_2)$^{1/2}$/(D^g for N_2-O_2)$^{1/2}$/(D^g for He-O_2)$^{1/2}$, of 1/1/1.9, indicating the validity of the previous postulation.

It may be reasonable to conclude, therefore, that the diffusion of oxygen gas through the gas film on the surface of the melt controls the rate of oxidation of liquid iron by the three gas mixtures containing less than 85 pct oxygen. Negligible effect of N_2 absorption might be due to the formation of an oxygen enriched surface layer on the melt which is well known to slow down the rate of N_2 absorption.[11,12] For the gas mixtures containing more than 85 pct oxygen, both chemical reaction and diffusion limit the rate, although the former begins to play a dominant role with increasing oxygen concentration in the mixtures.

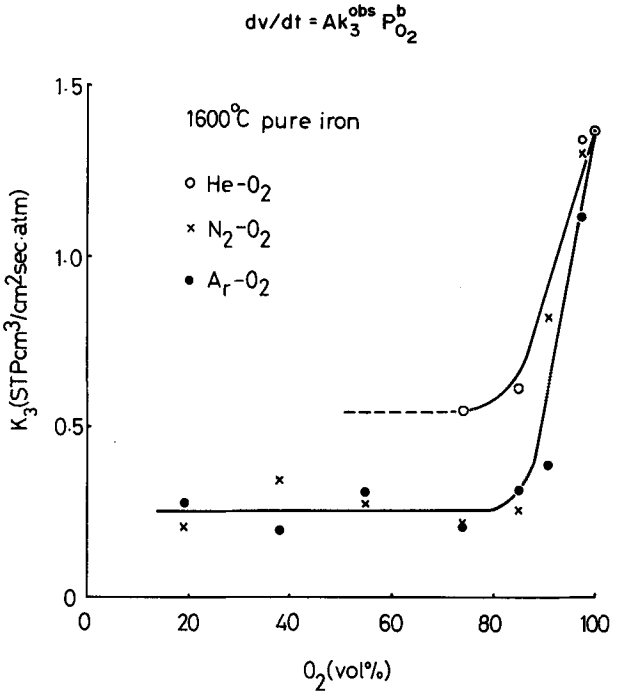

Fig. 6—Rate constants for diffusion controlled oxidation of liquid iron by oxygen bearing gas mixtures.

Table III. Observed Compared to Theoretical Ratio of Oxygen Transfer through Gaseous Boundary Layer

Parameters	Systems Ar-O_2	N_2-O_2	He-O_2
k_3^{obs}	0.26	0.26	0.55
$(D^g)^{1/2}$	1.26	1.26	2.35
k_3^{obs} ratio	1	1	2.1
$(D^g)^{1/2}$ ratio	1	1	1.9

k_3^{obs} and D^g are in units of STP$cm^3/cm^2 s \cdot atm$ and cm^2/s, respectively.

Rate-Controlling Steps as Displayed on Oxygen Gas Concentration-Alloy Composition Coordinates

A close examination of Figs. 5 and 6 can give a diagram on which one can locate which mechanism is dominant at what gas and metal compositions. Once a rate-limiting step is found at a desired composition of gas and metal, the corresponding rate constant is subsequently found in Figs. 5 and 6, or in the preceding sections of this article.

In Fig. 7, the ordinate is the concentration of alloying elements and the abscissa is the concentration of gaseous oxygen. If the rate of a step at one point on the diagram is less than about one-third of that of the other simultaneously working steps, then the former

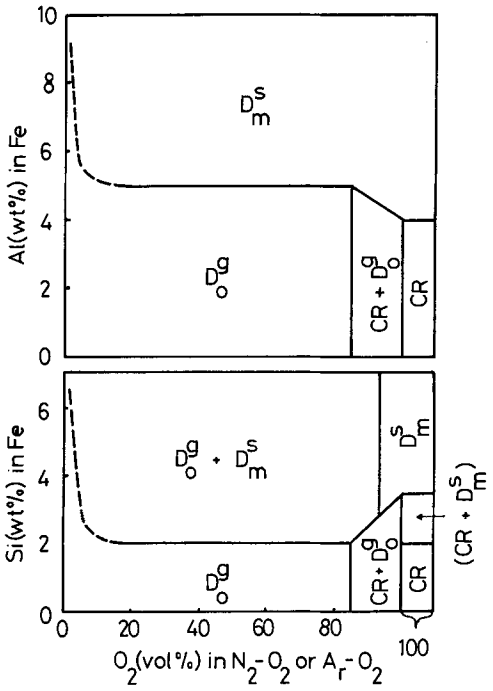

Fig. 7—Schematic representation of rate-controlling steps on oxygen concentration *vs* alloying element concentration coordinates.

Nomenclature:

CR = Chemical Reaction Control ($\frac{1}{2}O_2(g) \rightarrow O$ (oxide))

D_O^g = Diffusion Control of O_2 in the Boundary Layer within the Gas-Mixtures

D_m^s = Diffusion Control of Ions through the Surface Oxide Layer.

is considered to be a single rate-controlling step at that point. If the ratio is more than one-third, a mixed control of relevant steps is assigned to that point. The choice of one-third is of course arbitrary. Although in this case, the diagram is limited in part to the particular experimental arrangement, this form of presentation is suggested as a useful quick reference to determine the rate controlling step for gas-metallic alloy reactions.

CONCLUSIONS

Oxidation rates of pure iron melt by the mixtures of O_2 and He, N_2, or Ar, and that of Fe-Si or Fe-Al alloy melts by pure O_2 have been determined using a modified Sieverts' method.

Two distinct stages of oxidation were observed in every experiment; the first stage occurs immediately after the introduction of gases onto the surface of melts, and involves rapid exothermic chemical reactions between oxygen in gases and the surface of the melts. A subsequent second stage, where temperature resumes its initial value, then takes place, exhibiting much slower rates.

The effect of Si on the amount of O_2 consumed during the first stage is negligible up to 3 pct, then becomes significant around 4 pct beyond which a marked decrease of the amount is observed. The critical concentrations are 5 pct for Fe-Si and 8 pct for Fe-Al melts.

The effect of Si on the oxidation rate in the second stage is to decrease the rate constant linearly with increasing concentration up to about 4 pct, beyond which the rate constant reaches a constant low value. The effect of Al on the rate constant is negligible up to 4 pct, then beyond 5 pct the rate becomes virtually zero.

The amount of O_2 consumed from gas mixtures by iron melts during the first stage decreases markedly even with only 1 pct diluent in O_2, but continually decreases up to 80 pct diluent. The rate constant of oxidation by every mixture in the second stage decreases considerably up to 20 pct diluent, then exhibits a constant low value.

Theoretical considerations on the kinetics reveal that the oxidation of the alloy melts by pure oxygen gas is controlled by the diffusion of ions through oxide films formed on the surface of the melts, whereas that of a pure iron melt by a gas mixture containing less than 85 pct oxygen is limited by the diffusion of O_2 across the gaseous boundary layer at gas/melt interfaces.

These rate limiting steps are displayed on a diagram as a function of the concentration of the alloying elements in iron melts and that of diluents in gas mixtures.

ACKNOWLEDGMENT

The partial support of The American Iron and Steel Institute is gratefully acknowledged. The authors are thankful to Messieurs F. Bleicher, R. Marrone and D. Conliffe, and M. Small for X-ray analysis of surface oxides, computer programming for data analysis, and for a portion of the experimental work, respectively. They also wish to thank Mr. T. Sakuraya for carrying out some calculations.

REFERENCES

1. S. I. Filippov and S. Martynov: *Izv. Vysshikh Uchebn. Zavedenii Chem. Met.*, 1961, pp. 5-11.
2. R. Baker: *J. Iron Steel Inst.*, 1967, vol. 205, pp. 637-41.
3. R. S. Kaplan and W. O. Philbrook: *Trans. TMS-AIME*, 1969, vol. 245, pp. 2195-204.
4. Y. Kawai and K. Mori: *Tetsu-to-Hagane*, 1970, vol. 56, pp. 695-707.
5. N. Sano and Y. Matsushita: *Trans. I.S.I. Japan*, 1971, vol. 11, pp. 232-39.
6. D. G. C. Robertson and A. F. Jenkins: *Proc. Int. Conf. on Heterogeneous Kinetics at Elevated Temperatures*, pp. 393-408, Philadelphia, 1970.
7. T. Emi, W. M. Boorstein, and R. D. Pehlke: *Met. Trans.*, 1974, vol. 5, pp. 1959-66.
8. T. P. Hoar and L. E. Price: *Trans. Faraday Soc.*, 1938, vol. 34, p. 867.
9. W. A. Fisher and W. Ackermann: *Arch. Eisenhüttenw.*, 1968, vol. 39, pp. 273-76.
10. R. B. Bird, W. E. Stewart, and E. N. Lightfoot: *Transport Phenomena*, pp. 24, 511, and 746, Wiley, 1960.
11. R. D. Pehlke and J. F. Elliott: *Trans. TMS-AIME*, 1963, vol. 227, p. 844.
12. K. Suzuki, K. Mori, and Y. Ito: *Tetsu-to-Hagane*, 1969, vol. 55, pp. 877-86.